Identification of COL1A1 as an invasion-related gene in malignant astrocytoma

SHEN SUN[1,2*], YUE WANG[3*], YUE WU[3*], YUE GAO[3], QI LI[3], AYANLAJA ABIOLA ABDULRAHMAN[3], XIN-FENG LIU[3], GUANG-QUAN JI[3], JIN GAO[3], LI LI[4], FA-PING WAN[5], YUN-QING LI[6] and DIAN-SHUAI GAO[2,3]

[1]Department of Histology and Embryology; [2]National Demonstration Center for Experimental Basic Medical Science Education, Xuzhou Medical University; [3]Department of Neurobiology and Anatomy, Xuzhou Key Laboratory of Neurobiology, Jiangsu Key Laboratory of New Drug Research and Clinical Pharmacy, Xuzhou Medical University; [4]Department of Pathophysiology, Xuzhou Medical University; [5]Department of Human Anatomy, Xuzhou Medical University, Xuzhou, Jiangsu 221004; [6]Department of Anatomy and Histology, The Fourth Military Medical University, Xi'an, Shaanxi 710003, P.R. China

Received February 2, 2018; Accepted August 24, 2018

DOI: 10.3892/ijo.2018.4568

Abstract. Malignant astrocytoma (MA) is the most common and severe type of brain tumor. A greater understanding of the underlying mechanisms responsible for the development of MA would be beneficial for the development of targeted molecular therapies. In the present study, the upregulated differentially expressed genes (DEGs) in MA were obtained from the Gene Expression Omnibus database using R/Bioconductor software. DEGs in different World Health Organization classifications were compared using the Venny tool and 15 genes, including collagen type I α1 chain (COL1A1) and laminin subunit γ1 (LAMC1), were revealed to be involved in the malignant progression of MA. In addition, the upregulated DEGs in MA were evaluated using functional annotations of Gene Ontology and Kyoto Encyclopedia of Genes and Genomes with the Database for Annotation, Visualization, and Integrated Discovery tool. The results indicated that invasion-associated enrichment was observed in 'extracellular matrix' (ECM), 'cell adhesion' and 'phosphoinositide 3-kinase-protein kinase B signaling pathway'. Subsequently, the analysis of the protein-protein interactions was performed using STRING and Cytoscape software, which revealed that the ECM component was the invasion-associated module and its corresponding genes included COL1A1, LAMC1 and fibronectin 1. Finally, survival Kaplan-Meier estimate was conducted using cBioportal online, which demonstrated that COL1A1 expression affected the survival of and recurrence in patients with MA. Moreover, the results of *in vitro* Transwell assay and western blot analysis revealed that the depleted levels of COL1A1 also decreased the expression of several proteins associated with cell invasion, including phosphorylated-signal transducer and activator of transcription 3, matrix metalloproteinase (MMP)-2, MMP-9 and nuclear factor-κB. On the whole, the present study identified the invasion-related target genes and the associated potential pathways in MA. The results indicated that COL1A1 may be a candidate biomarker for the prognosis and treatment of MA.

Correspondence to: Dr Dian-Shuai Gao, Department of Neurobiology and Anatomy, Xuzhou Key Laboratory of Neurobiology, Jiangsu Key Laboratory of New Drug Research and Clinical Pharmacy, Xuzhou Medical University, 209 Tongshan Road, Xuzhou, Jiangsu 221004, P.R. China
E-mail: gds@xzhmu.edu.cn

*Contributed equally

Key words: bioinformatics, malignant astrocytoma, invasion, extracellular matrix, collagen type I α1 chain, laminin subunit γ1

Introduction

Gliomas are the most common type of primary brain tumor in adults; malignant glioma in the brain mainly is referred to as astrocytoma [World Health Organization (WHO) III] and glioblastoma (GBM; WHO IV) (1). Despite the optimal treatments available, the 5-year relative survival rate is only 4.7% for patients with GBM and 25.9% for patients with astrocytoma, which is less than the rates associated with other types of glioma (2). One of the most likely explanations for the low survival rate and high levels of recurrence in malignant astrocytoma (MA) may be its diffuse infiltrative nature (1). Therefore, gaining a greater understanding of the molecular mechanisms underlying the invasive phenotypes of MA is crucial for the development of novel treatment strategies for MA.

To date, a number of modern technologies have been developed that have provided new opportunities for the identification of novel strategies and biomarkers for cancer diagnosis, therapies and prognosis (3). Bioinformatics, including nucleic acid sequence analysis, protein sequence analysis and genomics, can be used to collect, process, store, classify, analyze and interpret biological information through

the application of mathematics and computer technology. For example, when combined with microarray technology, bioinformatics analysis can identify the connection between meaningful molecular interactions and evaluate the associated signaling pathways (4).

In the present study, high-throughput data were downloaded from online databases, which were then analyzed through bioinformatics methods using R language, Database for Annotation, Visualization, and Integrated Discovery (DAVID), STRING and Cytoscape software. Survival analysis was then performed using public statistical data in order to identify the malignant progression-associated biomarkers of MA. Additional experimental approaches were also performed in order to validate these results.

In this study, the collagen type I α1 (*COL1A1*) gene was identified as a invasion-related gene from bioinformatics analysis. The α1 chain of type I collagen, encoded by the *COL1A1* gene, the major extracellular matrix (ECM) component, has been reported in multiple types of cancer, including GBM (5,6) and has been reported to be involved in multiple biological behaviors, including cell proliferation, invasion, metastasis and angiogenesis (7,8). In this study, using bioinformatics intervention, we made a firm confirmation of the high level of expression of COL1A1 in MA, which may have an impact on the survival rate of patients.

Materials and methods

Microarray data. Gene Expression Omnibus (GEO; http://www.ncbi.nlm.nih.gov/geo) is a public repository for data storage, such as microarray and next-generation sequencing, which is open access and freely available. The GSE4290, GSE15824 and GSE19728 datasets were used to download expression data, including different grades (WHO) of astrocytoma and normal brain data. In the present study, the platform used to collect the microarray data was all based on the GPL570 [HG-U133_Plus_2] Affymetrix Human Genome U133 Plus 2.0 Array (9). In the GSE4290 data series, there were 23 samples from patients with epilepsy, which were used as non-tumor samples in the present study, and 26 astrocytoma and 81 GBM samples, which were used as the tumor samples (10). The GSE15824 series included 19 frozen human glioma tissue samples and 2 normal brain samples that were obtained during surgery, which were processed according to the guidelines of the Ethics Committee of the University Hospitals of Basel (11). The GSE19728 series comprised total RNA that was isolated from 17 patient tumor tissues and 4 pooled samples of normal tissue (12).

Data processing and identification of differentially expressed genes (DEGs). R is a well-designed open source language that is essential for data analysis and visualization. The R-based packages provide a broad range of statistical and graphical techniques (13). The above probe-level data (.cel files) were processed using R language, which included the use of affy package, an R package for the analysis of oligonucleotide arrays manufactured by Affymetrix; Thermo Fisher Scientific, Inc. (Waltham, MA, USA) (9), and the MAS5 algorithm, a well-known pre-processing technique (14). To analyze the upregulated DEGs between the high-grade glioma and normal brain groups in each microarray dataset, a classical t-test with a cut-off criterion of $P<0.05$ and a fold control (FC) of ≥2.0 were used. To evaluate the different interactions between the upregulated DEGs, Venny's online software (http://bioinfogp.cnb.csic.es/tools/venny/index.html) was used to draw Venn diagrams. Furthermore, where necessary, the present study used the GeneChip® Human Genome U133 Plus 2.0 Array (http://www.affymetrix.com/estore/index.jsp) to generate the gene expression profiling datasets annotated from the raw data.

Gene Ontology (GO) and Kyoto Encyclopedia of Genes and Genomes (KEGG) pathway enrichment analysis of DEGs. GO is an updated, comprehensive, major bioinformatics system that facilitates high-quality functional gene annotation for all species (15,16). KEGG (http://www.genome.jp/) is an online encyclopedia of genes and genomes that provides information associated with genomes, metabolism, biological pathways, diseases and chemical substances (17). DAVID (http://www.david.niaid.nih.gov) is an online platform that provides query-based access. It integrates biologically rich information from large datasets and displays graphic summaries of functional information (18). The present study uploaded the DEGs to DAVID and used the functional annotation tool to perform GO and KEGG pathway enrichment analysis ($P<0.01$).

Integration of protein-protein interaction (PPI) network and module analysis. The STRING database (http://string-db.org) is an online network that critically assesses protein-protein, direct (physical) or indirect (functional), interactions (19). The present study input the DEGs on STRING in order to obtain the PPI network from it (medium confidence: 0.400). Subsequently, the PPI network was constructed using Cytoscape software (http://www.cytoscape.org). Cytoscape is a type of software environment for visualizing molecular interaction networks and biological pathways, with annotations, gene expression profiles and other datasets (20). The present study used 3 plugins of Cytoscape; MCODE, ClueGo and CluePedia. MCODE is a Cytoscape application that clusters a given network based on topology in order to produce highly interconnected subgraphs of molecular complexes and parts of pathways (21). ClueGO is a Cytoscape plug-in that can divide large clusters of genes into functional groups based on GO, KEGG, Wiki Pathways and Reactome (22). CluePedia is a ClueGO plugin that can integrate information regarding genes, proteins and microRNAs into a network with ClueGO terms/pathways (23).

In the present study, MCODE was used to create clusters. The main parameters were as follows: Fluff; Degree Cutoff = 2; Node Density Cutoff = 0.1; node score cutoff = 0.2; K-Core = 2; and Maximum Depth = 100. Subsequently, the ClueGo and Cluepedia plug-ins were used in combination to analyze the clusters and visualize the functional groups based on GO and KEGG, as well as the genes associated with these groups. The evidence codes used were as follows: #Genes in KEGG, GO_MF, GO_CC and GO_BP; $P<0.05$.

Analysis of protein expression. To determine the protein expression levels of the corresponding genes in MA, the present study referred to the Human Protein Atlas available from www.proteinatlas.org (24).

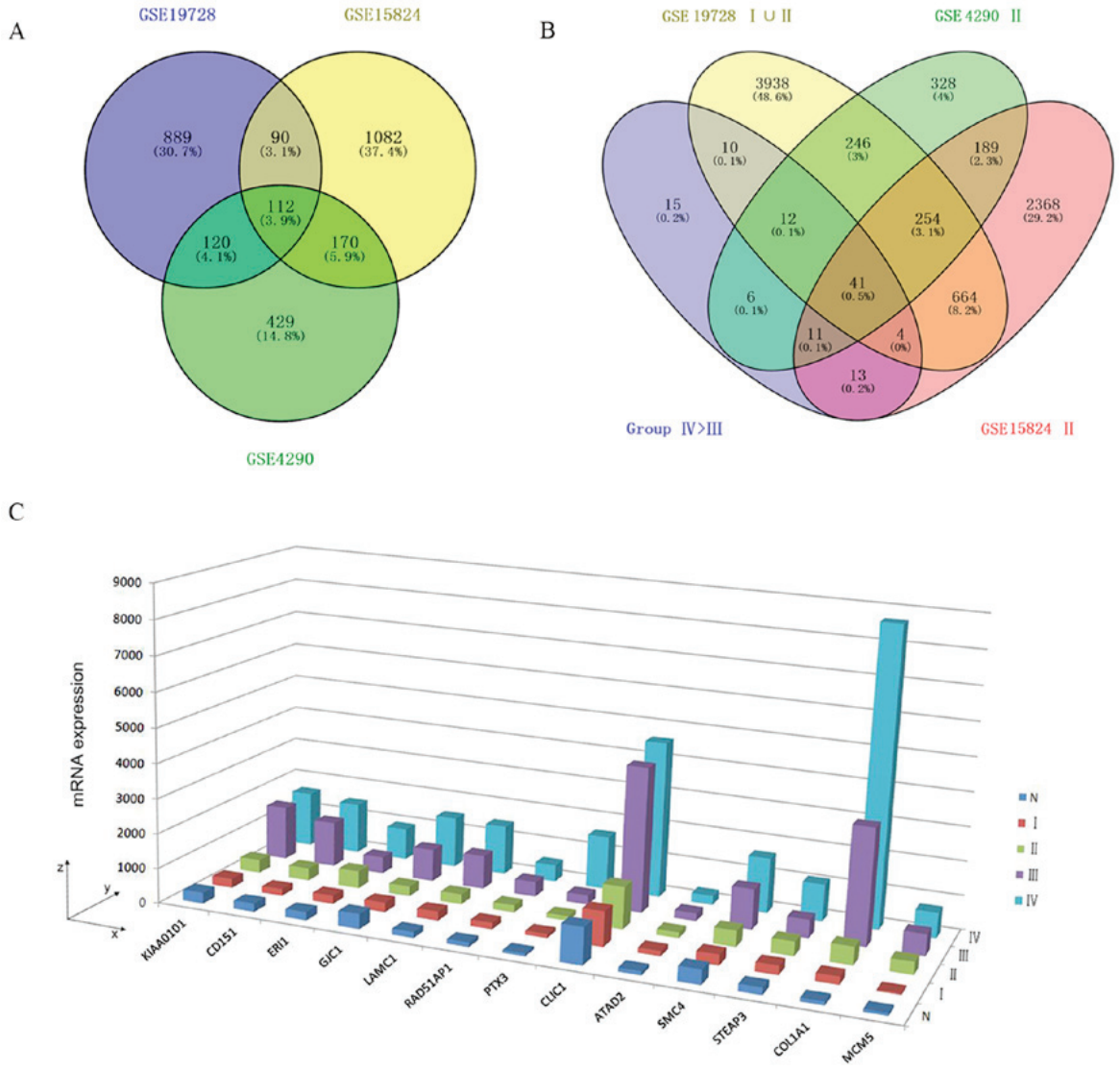

Figure 1. MA-related upregulated DEGs. (A) A 3-set Venn diagram presenting the intersection between upregulated DEGs of high-grade astrocytoma ($FC_{IV} > FC_{III}$) from the GSE4290, GSE19728 and GSE15824 microarrays. (B) A 4-set Venn diagram presenting the intersection between upregulated DEGs of Group IV>III, including GSE4290 II, GSE15824 II and GSE19728 I∪II. (C) Three-dimensional histogram presenting the mRNA expression of DEGs from Group IV>III, no I or II, in GSE19728. x-axis, official gene symbols; y-axis, WHO grades IV, III, II and I and normal brain (N); z-axis, mRNA expression values. MA, malignant astrocytoma; DEGs, differentially expressed genes; WHO, World Health Organization.

Survival analysis of DEGs. The Cancer Genome Atlas (TCGA; http://cancergenome.nih.gov/) is a comprehensive, multi-dimensional map of the key genomic changes in 33 types of cancer. The cBioPortal for Cancer Genomics is a user-friendly, open-access web platform for the visualization, analysis, and download of large-scale cancer genomics datasets (25). To evaluate the effects of the selected DEGs on the survival of patients with MA, GBM Multiforme (TCGA, Provisional) datasets were selected to generate the overall survival (OS) and disease-free survival (DFS) Kaplan-Meier (KM) plots using the cBioPortal online platform. In total, 166 tumor samples with mRNA data (RNA-Seq V2) were selected as the patient dataset and the mRNA expression z-Scores (RNA-Seq V2 RSEM) were selected as the genomic profile ($P<0.05$).

Cell lines and culture. The human astrocytoma cell line, U251MG, and the GBM of unknown origin cell line, U87MG (authenticated by STR profiling), were maintained in Dulbecco's modified Eagle's medium (DMEM; 1X High Glucose; Gibco/Thermo Fisher Scientific, Inc.) supplemented with 10% fetal bovine serum (FBS; Gibco/Thermo Fisher Scientific, Inc.) at 37˚C and 5% CO_2. The U251MG and U87MG cells were used for stable transfection with siRNA directed against COL1A1, which were was obtained from GenePharma (Shanghai). U251MG and U87MG cells that were cultured with the COL1A1 siRNA used as the experimental group were named as 'COL1A1 siRNA' cells. U251MG and U87MG cells with the treatment of siControl served as the control group were designated as 'Non-targeted' or 'NT' cells. The growth medium was replenished every 4 days until >80% cells reached confluence.

COL1A1 gene silencing. siRNA were purchased from GenePharma (Shanghai, China). The sequences of the targeting siRNA and the control were as follows: siRNA

Table I. Top 10 terms of biological processes (BP).

Category	Term	Description	P-value	Gene
GOTERM_BP_DIRECT	GO:0030198	Extracellular matrix organization	1.88E-09	COL1A1, CD44, COL3A, COL4A1, COL4A2, FN1, GFAP, ITGB2, LAMB2, LAMC1, NID1, TNC
GOTERM_BP_DIRECT	GO:0006958	Complement activation, classical pathway	1.89E-06	C1QA, C1QB, C1QC, C1RL, C1R, C1S, C3
GOTERM_BP_DIRECT	GO:0050776	Regulation of immune response	9.80E-06	TYROBP, COL1A1, COL3A1, C3, ITGB2, HLA-B, HLA-C, HLA-F
GOTERM_BP_DIRECT	GO:0006956	Complement activation	1.56E-05	C1QA, C1QB, C1QC, C1R, C1S, C3
GOTERM_BP_DIRECT	GO:0060333	Interferon-γ-mediated signaling pathway	2.07E-05	CD44, GBP1, GBP2, HLA-B, HLA-C
GOTERM_BP_DIRECT	GO:0045087	Innate immune response	3.45E-05	TYROBP, C1QA, C1QB, C1QC, C1RL, C1R, C1S, HLA-B, HLA-C, PTX3, RNF135
GOTERM_BP_DIRECT	GO:0009611	Response to wounding	2.94E-04	ZFP36L2, F2R, FN1, GFAP, TNC
GOTERM_BP_DIRECT	GO:0002480	Antigen processing and presentation of exogenous peptide antigen via MHC class I, TAP-independent	7.71E-04	HLA-B, HLA-C, HLA-F
GOTERM_BP_DIRECT	GO:0006955	Immune response	7.94E-04	FYB, TNFRSF1A, C1QC, C1R, C3, GBP2, HLA-B, HLA-C, HLA-F
GOTERM_BP_DIRECT	GO:0007155	Cell adhesion	0.001423	CD151, CD44, COL1A1, FN1, IGFBP7, ITGB2, 22LAMB2, LAMC1, TNC

sense (5'-3'), CAUUGGUAAUGUUGGUGCUTT and antisense (5'-3'), AGCACCAACAUUACCAAUGTT; and control sense (5'-3'), UUCUCCGAACGUGUCACGUTT and antisense (5'-3'), ACGUGACACGUUCGGAGAATT. The synthesized siRNAs were transfected into the U251 or U87 cells using Lipofectamine 2000 according to the manufacturer's instructions. Briefly, (1.5-2)x10^5 U251 or U87 glioma cells were seeded in 6-well plates for 24 h. siRNA dissolved in serum free-medium was incubated for 20 min at room temperature. The cells were then replaced with fresh medium containing 25 nM siRNA, and then cultured for specific periods of time (24 h) for further analysis.

Invasion assay. Cell invasion assays were performed using Transwell with Matrigel-coated membrane filter inserts in 24-well culture plates (Corning Inc., Corning, NY, USA). The U251MG and U87MG cells were seeded at a density of 1x10^4 cells in 200 μl of serum-free medium in the upper chamber. The bottom chamber was fixed with 600 μl of culture medium containing 10% FBS and 1% penicillin streptomycin (Thermo Fisher Scientific, Inc.). The cells on the lower surface of the membrane were fixed with 4% formaldehyde and stained with crystal violet (Vicmed Biotech Co., Ltd., Xuzhou, China). The stained invaded cells were photographed under an inverted light microscope (magnification, x100; Olympus Corp., Tokyo, Japan) and counted in 5 random fields of view.

Western blot analysis. The matrix metalloproteinase (MMP)-2, MMP-9, nuclear factor (NF)-κB and phosphorylated-signal transducer and activator of transcription 3 (p-STAT3) protein levels were determined by western blot analysis. Briefly, cells were collected following treatment with COL1A1 siRNA for 24 h, and cell lysates were prepared in 10 mm Tris (pH 7.5), 1 mm EDTA, 400 mm NaCl, 10% glycerol, 0.5% NP40, 5 mm NaF, 0.5 mm sodium vanadate, 1 mm DTT and 0.1 mm phenylmethylsulfonyl fluoride. Proteins extracted from the experimental and control groups were denatured, electrophoretically separated by 8% SDS-PAGE and transferred onto nitrocellulose membranes (EMD Millipore, Billerica, MA, USA). After blocking with 5% non-fat milk, the membranes were incubated overnight at 4˚C with the following primary antibodies: MMP-2 (10373-2-AP, 1:500; ProteinTech Group, Inc., Chicago, IL, USA), MMP-9 (10375-2-AP, 1:500; ProteinTech Group, Inc.), pSTAT3 (CJ44121, 1:500; Bioworld Technology, Co., Ltd., Nanjing, China) and NF-κB (MA D14E12, 1:1,000; Cell Signaling Technology, Inc., Danvers, MA, USA). Anti-β-actin (1:10,000; Santa Cruz Biotechnology, Inc., Dallas, TX, USA) was used as a protein loading control. The blots were then incubated for 2 h with goat anti-rabbit (Lot No. C60321-05) or goat anti-mouse (Lot No. C70124-05) secondary antibodies, respectively (1:1,000; LI-COR Biosciences, Lincoln, NE, USA). All the protein bands were scanned using the Odyssey Infrared laser scanning image system (LI-COR Biosciences) once washed. The bands on the membranes were analyzed

Table II. Top 10 terms of molecular function (MF).

Category	Term	Description	P-value	Gene
GOTERM_MF_DIRECT	GO:0005201	Extracellular matrix structural constituent	3.10E-04	COL1A1, COL3A1, COL4A1, COL4A2, LAMC1
GOTERM_MF_DIRECT	GO:0004252	Serine-type endopeptidase activity	9.49E-04	C1QA, C1QB, C1QC, C1RL, C1R, C1S, C3
GOTERM_MF_DIRECT	GO:0048407	Platelet-derived growth factor binding	1.24E-03	COL1A1, COL3A1, COL4A1
GOTERM_MF_DIRECT	GO:0005102	Receptor binding	1.60E-03	ABCA1, FYB, TYROBP, F2R, C3, IDH1, HLA-B, HLA-F
GOTERM_MF_DIRECT	GO:0005178	Integrin binding	1.68E-03	CD151, COL3A1, FN1, GFAP, LAMB2
GOTERM_MF_DIRECT	GO:0001948	Glycoprotein binding	3.52E-03	FLNA, GFAP, ITGB2, VIM
GOTERM_MF_DIRECT	GO:0005515	Protein binding	3.78E-03	ABCA1, BARD1, CD151, CD163, DAB2, FYB, KIAA0101, RAB13, RAD51AP1, STEAP3, TEAD1, THOC2, TNFRSF1A, TYROBP, ZFP36L2, ANXA2, CALU, CHEK1, CLIC1, F2R, COL1A1, COL3A1, C3, CDK1, DTX3L, FN1, FLNA, GFAP, GBP1, HMG20B, IGFBP7, ITGB2, MCCC2, MCM5, MYOF, NOTCH2NL, PTX3, PTBP1, PTPRC, RNF135, SLC40A1, UHRF1, VIM
GOTERM_MF_DIRECT	GO:0042605	Peptide antigen binding	1.05E-02	HLA-B, HLA-C, HLA-F
GOTERM_MF_DIRECT	GO:0098641	Cadherin binding involved in cell-cell adhesion	1.33E-02	ARHGAP18, ANXA2, CALD1, CLIC1, FLNA, IDH1
GOTERM_MF_DIRECT	GO:0046977	TAP binding	0.014459	HLA-B, HLA-C

using ImageJ 1.48v software (National Institutes of Health, Bethesda, MD, USA).

Statistical analysis. All data were analyzed with SPSS 16.0 software (SPSS, Inc., Chicago, IL, USA) and are expressed as the means ± standard deviation. Independent sample t-tests were conducted to identify significant differences in the mean values between the two groups. One-way analysis of variance was performed to compare the mean values of multiple samples. The post hoc LSD and S-N-K tests were used for the comparison of the means of the control versus the case groups. A value of $P<0.05$ was considered to indicate a statistically significant difference.

Results

Identification of MA-related upregulated DEGs. The Venn diagram revealed that the intersection between the upregulated DEGs in the high-grade astrocytoma cases ($FC_{IV} > FC_{III}$) from the GSE4290, GSE19728 and GSE15824 datasets was 112 (Fig. 1A; termed group IV>III). Once the DEGs from the samples with WHO grades I or II were removed, there were 15 DEGs remaining (termed group 'IV>III, with no I or II'; Fig. 1B and C), including PCNA clamp associated factor (*PCLAF*, also known as *KIAA0101*), cluster of differentiation 151 (*CD151*), exoribonuclease 1 (*ERI1*), gap junction protein γ1 (*GJC1*), laminin subunit γ1 (*LAMC1*), RAD51 associated protein 1 (*RAD51AP1*), pentraxin 3 (*PTX3*), chloride intracellular channel protein 1 (*CLIC1*), ATPase family, AAA domain containing 2 (*ATAD2*), structural maintenance go chromosome 4 (*SMC4*), six-transmembrane epithelial antigen of prostate 3 (*STEAP3*), COL1A1 and minichromosome maintenance complex component 5 (*MCM5*).

GO term enrichment and KEGG pathway analysis. Using the online software, DAVID, the DEGs of group IV>III were annotated and the overrepresented GO terms and KEGG pathways were identified. The results revealed that these DEGs were significantly enriched in biological processes (BP), including 'extracellular matrix (ECM) organization' and 'cell adhesion' (Table I). For molecular function (MF), the upregulated DEGs might be enriched in 'ECM structural constituent' (Table II). In addition, the cell component (CC) analysis demonstrated that the upregulated DEGs were significantly enriched in terms associated with extracellular functions, such as extracellular exosome and extracellular matrix (Table III). Furthermore, using the gene annotation tool for the KEGG pathway, the upregulated DEGs might be enriched in 'ECM-receptor interaction', 'Focal adhesion' and 'phosphoinositide 3 (PI3K)-kinase-protein kinase B (Akt) signaling pathway' (Table IV).

Table III. Top 10 terms of cell component (CC).

Category	Term	Description	P-value	Gene
GOTERM_CC_DIRECT	GO:0005576	Extracellular region	7.98E-10	CD163, TNFRSF1A, APOC1, CALU, F2R, COL1A1, COL3A1, COL4A1, COL4A2, C1QA, C1QB, C1QC, C1R, C1S, C3, FN1, FLNA, GBP1, IGFBP7, LAMB2, LAMC1, HLA-C, NID1, NOTCH2NL, PTX3, PLTP, TNC, TFPI
GOTERM_CC_DIRECT	GO:0031012	Extracellular matrix	9.55E-09	ANXA2, COL1A1, COL3A1, COL4A1, COL4A2, FN1, FLNA, IGFBP7, LAMB2, LAMC1, NID1, TNC, VIM
GOTERM_CC_DIRECT	GO:0070062	Extracellular exosome	6.04E-07	ATAD2, CD44, DAB2, FCGR2A, RAB13, ANXA2, APOC1, CLIC1, COL4A2, C1QA, C1QB, C1QC, C1RL, C1R, C1S, C3, CDK1, FN1, FLNA, IGFBP7, ITGB2, IDH1, LAMB2, LAMC1, HLA-B, HLA-C, MYOF, NID1, PTBP1, PSMB9, PTPRC, VIM
GOTERM_CC_DIRECT	GO:0005604	Basement membrane	1.99E-06	CD151, ANXA2, COL4A1, LAMB2, LAMC1, NID1, TNC
GOTERM_CC_DIRECT	GO:0072562	Blood microparticle	4.90E-05	CLIC1, C1QB, C1QC, C1R, C1S, C3, FN1
GOTERM_CC_DIRECT	GO:0005581	Collagen trimer	5.93E-05	COL1A1, COL3A1, C1QA, C1QB, C1QC, MSR1
GOTERM_CC_DIRECT	GO:0009986	Cell surface	2.05E-04	CD44, TNFRSF1A, TYROBP, ANXA2, F2R, ITGB2, HLA-B, HLA-C, HLA-F, PTPRC, TFPI
GOTERM_CC_DIRECT	GO:0005615	Extracellular space	3.27E-04	TNFRSF1A, ANXA2, CHEK1, CLIC1, COL1A1, COL3A1, C1QC, C1RL, C3, FN1, IGFBP7, LAMC1, PTX3, PLTP, PTPRZ1, TNC, TFPI
GOTERM_CC_DIRECT	GO:0042612	MHC class I protein complex	1.51E-03	HLA-B, HLA-C, HLA-F
GOTERM_CC_DIRECT	GO:0005605	Basal lamina	0.002026	FN1, LAMB2, NID1

Module screening from the PPI network. The DEGs of group IV>III were input into STRING online and the acquired interaction network of DEGs was then reconstructed to form the network using Cytoscape-MCODE. The results revealed that there were 2 clusters (Fig. 2). Further Cytoscape-ClueGo/CluePedia analysis demonstrated that in cluster 1, there were mainly 4 functional modules enriched such as 'ECM component' and 'collagen trimer' and the corresponding genes included *COL1A1*, *LAMC1* and fibronectin 1 (*FN1*) (Fig. 3).

COL1A1 and LAMC1 are overexpressed in human MA. By searching the Human Protein Atlas, the present study revealed that in some patients with MA, there was a positive expression of COL1A1 or LAMC1 in the tumor cells, while in the normal cerebral cortex, there was no positive staining of COL1A1 or LAMC1 in glial cells (Fig. 4).

KM plots. Comparisons between the cases with and without alterations in Query Genes, OS and DFS KM estimates were then made. The results revealed that in GBM, *COL1A1* was altered in 8 of the queried samples, while its OS (Fig. 5A) and DFS KM plots (Fig. 5B) both exhibited significant differences (P<0.05). *LAMC1*, on the other hand, was altered in 6 of the queried samples, and neither of its OS (Fig. 5C) nor DFS KM plots (Fig. 5D) exhibited significant differences (P>0.05). However, in brain Lower Grade Glioma (LGG), both *COL1A1* and *LAMC1* exhibited significant differences in the OS and DFS KM plots (Fig. 5E-H).

COL1A1 promotes glioma cell invasion. The effects of COL1A1 on U251MG or U87MG cell invasion were quantitatively determined by Transwell assay (Fig. 6). The investigated COL1A1 siRNA-treated groups exhibited an unequivocal decrease in their invasive capacities relative to the control cells (P<0.001).

Downregulation of COL1A1 may lead to a reduction in the levels of recognized invasion-related factors. A comparison between the results of western blot analysis (Fig. 7) and those

Table IV. Top 10 terms of KEGG pathway.

Category	Term	Description	P-value	Gene
KEGG_PATHWAY	hsa05150	*Staphylococcus aureus* infection	5.89E-08	FCGR2A, C1QA, C1QB, C1QC, C1R, C1S, C3, ITGB2
KEGG_PATHWAY	hsa04512	ECM-receptor interaction	9.60E-08	CD44, COL1A1, COL3A1, COL4A1, COL4A2, FN1, LAMB2, LAMC1, TNC
KEGG_PATHWAY	hsa04610	Complement and coagulation cascades	3.33E-07	F2R, C1QA, C1QB, C1QC, C1R, C1S, C3, TFPI
KEGG_PATHWAY	hsa05146	Amoebiasis	6.22E-06	COL1A1, COL3A1, COL4A1, COL4A2, FN1, ITGB2, LAMB2, LAMC1
KEGG_PATHWAY	hsa05133	Pertussis	1.01E-05	C1QA, C1QB, C1QC, C1R, C1S, C3, ITGB2
KEGG_PATHWAY	hsa04510	Focal adhesion	6.30E-05	COL1A1, COL3A1, COL4A1, COL4A2, FN1, FLNA, LAMB2, LAMC1, TNC
KEGG_PATHWAY	hsa04145	Phagosome	6.80E-05	FCGR2A, C1R, C3, ITGB2, MSR1, HLA-B, HLA-C, HLA-F
KEGG_PATHWAY	hsa05322	Systemic lupus erythematosus	2.66E-04	FCGR2A, C1QA, C1QB, C1QC, C1R, C1S, C3
KEGG_PATHWAY	hsa05020	Prion diseases	0.001395	C1QA, C1QB, C1QC, LAMC1
KEGG_PATHWAY	hsa04151	PI3K-Akt signaling pathway	0.002024	F2R, COL1A1, COL3A1, COL4A1, COL4A2, FN1, LAMB2, LAMC1, TNC

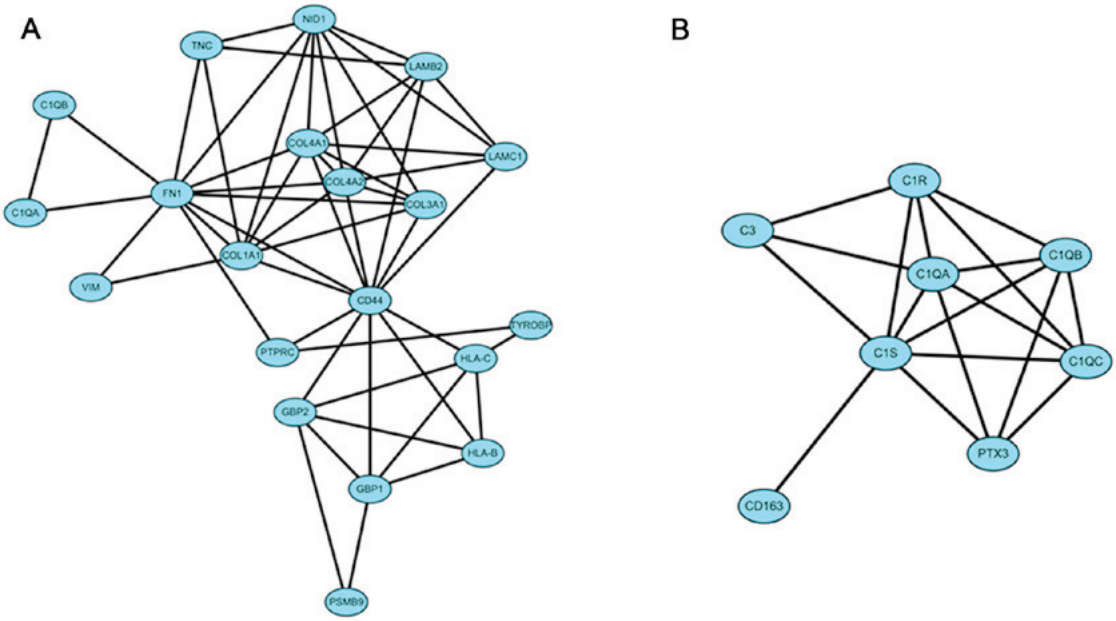

Figure 2. Cytoscape protein interaction analysis of differentially expressed genes. STRING interaction network of DEGs of 'Group IV>III' was analyzed by Cytoscape software. Using Plug-in MCODE, the network is divided into 2 clusters: (A) Cluster 1: Score=6, Nodes=11, Edges=30, the CD44 is the 'seed'; (B) Cluster 2: Score=65.6, Nodes=6, Edges=140, PTX3 is the 'seed'.

of the invasion assay (Fig. 6) indicated that, as was expected, the cells transfected with COL1A1 siRNA expressed lower levels of p-STAT3 (up to 60%) when compared with the endogenous levels in the U251MG or U87MG control cells. As shown in Fig. 7, the COL1A1 siRNA-transfected glioma cells exhibited a significant decrease (up to 60%) in the MMP-2 and MMP-9 protein levels. Furthermore, the expression of NF-κB in the COL1A1 siRNA-transfected group was significantly lower (up to 50%) than that observed in the NT group (Fig. 7).

Discussion

The development and progression of malignant glioma are driven by a series of genomic alterations, including changes in mRNA expression (26). Understanding the molecular mechanisms associated with malignant glioma is crucial for its diagnosis and treatment. Since microarrays and high-throughput sequencing can provide the expression levels of thousands of genes in the human genome simultaneously, they are now widely used to identify the potential therapeutic targets for MA (27).

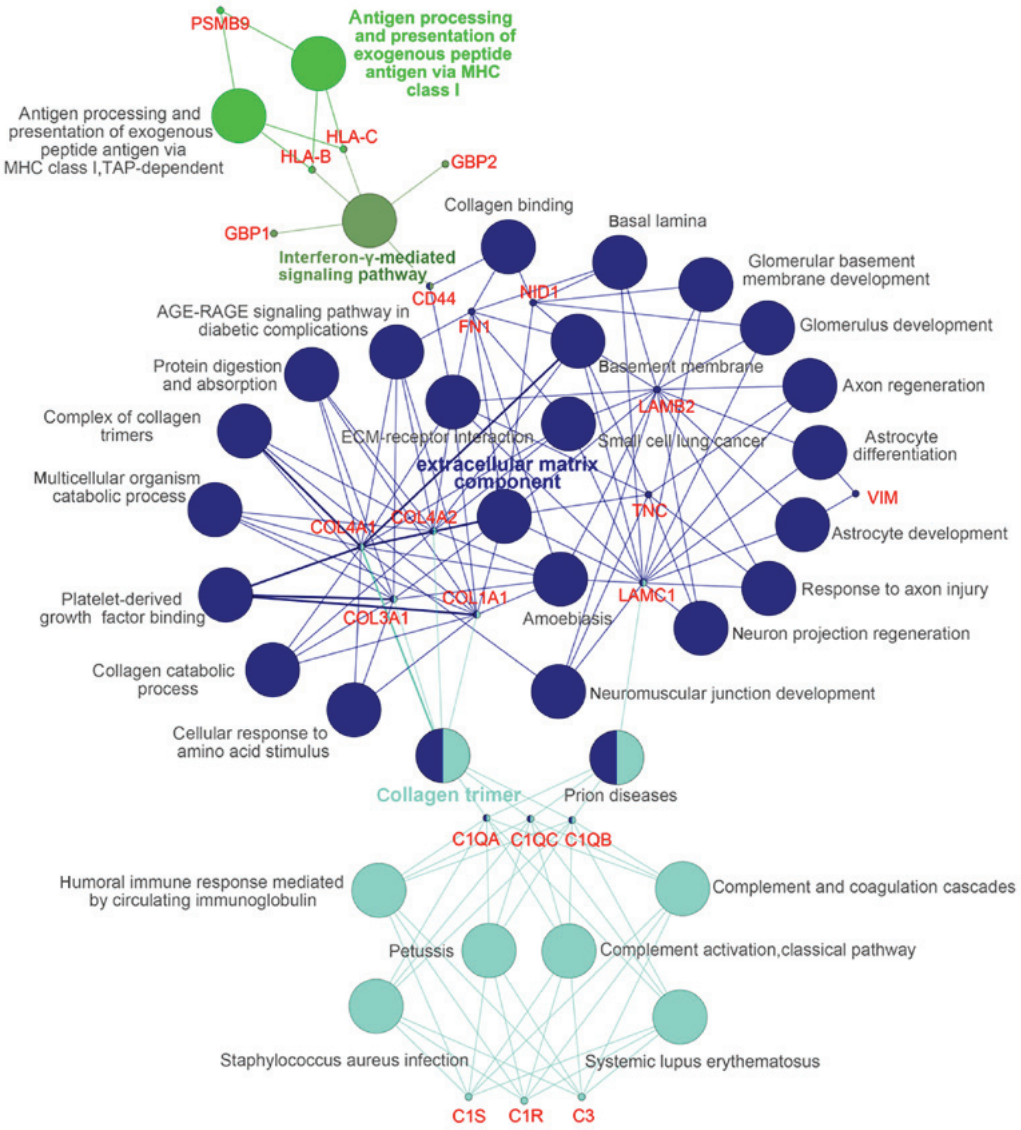

Figure 3. Cytoscape-ClueGo/CluePedia diagram presenting the protein-protein interaction of cluster 2 from Group IV>III.

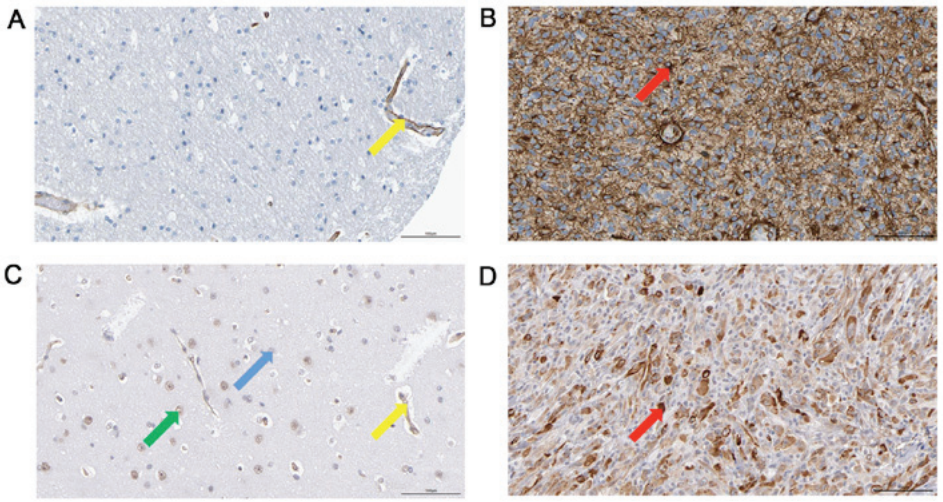

Figure 4. Immunohistochemical staining reveals that the protein expression of COL1A1/LAMC1 is upregulated in MA. (A) In the cerebral cortex, COL1A1 expression is only observed in endothelial cells (indicated by yellow arrow). Patient ID: 2927. (B) In MA, COL1A1 expression is observed in tumor cells (indicated by red arrow). Patient ID: 3241. (C) In the cerebral cortex, LAMC1 expression is observed in the endothelial cells (indicated by yellow arrow) and neuronal cells (indicated by green arrow). There is no LAMC1 expression in glial cells (indicated by blue arrow). Patient ID: 1539. (D) In MA, LAMC1 expression is observed in tumor cells (indicated by red arrow). Patient ID: 183. COL1A1, collagen type I α1; LAMC1, laminin subunit γ1; MA, malignant astrocytoma.

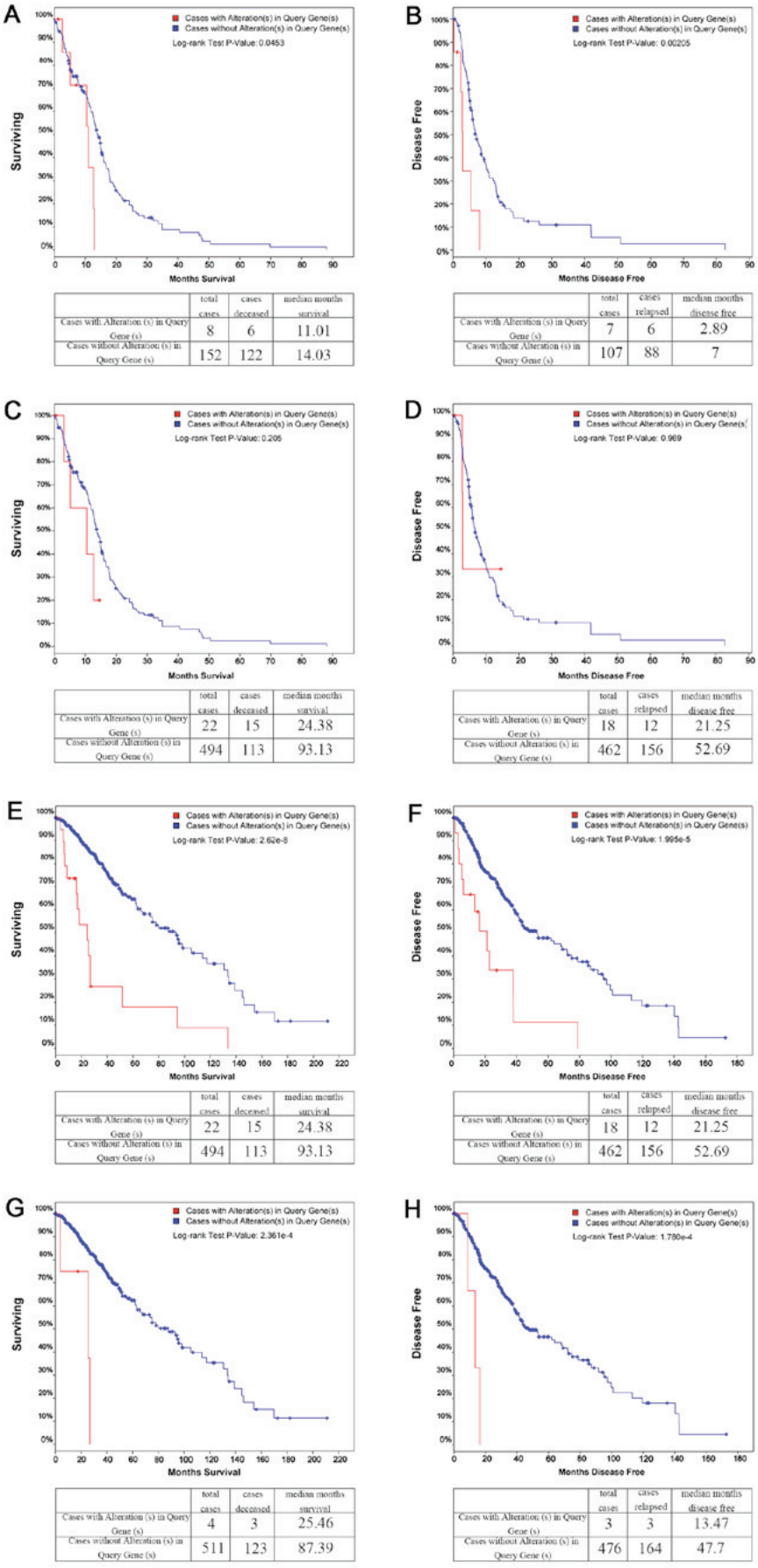

	total cases	cases deceased	median months survival
Cases with Alteration (s) in Query Gene (s)	8	6	11.01
Cases without Alteration (s) in Query Gene (s)	152	122	14.03

	total cases	cases relapsed	median months disease free
Cases with Alteration (s) in Query Gene (s)	7	6	2.89
Cases without Alteration (s) in Query Gene (s)	107	88	7

	total cases	cases deceased	median months survival
Cases with Alteration (s) in Query Gene (s)	22	15	24.38
Cases without Alteration (s) in Query Gene (s)	494	113	93.13

	total cases	cases relapsed	median months disease free
Cases with Alteration (s) in Query Gene (s)	18	12	21.25
Cases without Alteration (s) in Query Gene (s)	462	156	52.69

	total cases	cases deceased	median months survival
Cases with Alteration (s) in Query Gene (s)	22	15	24.38
Cases without Alteration (s) in Query Gene (s)	494	113	93.13

	total cases	cases relapsed	median months disease free
Cases with Alteration (s) in Query Gene (s)	18	12	21.25
Cases without Alteration (s) in Query Gene (s)	462	156	52.69

	total cases	cases deceased	median months survival
Cases with Alteration (s) in Query Gene (s)	4	3	25.46
Cases without Alteration (s) in Query Gene (s)	511	123	87.39

	total cases	cases relapsed	median months disease free
Cases with Alteration (s) in Query Gene (s)	3	3	13.47
Cases without Alteration (s) in Query Gene (s)	476	164	47.7

Figure 5. OS and DFS Kaplan-Meier estimate and relevant statistical table of COL1A1 and LAMC1 in GBM and LGG. (A) OS of COL1A1 in GBM; (B) DFS of COL1A1 in GBM; (C) OS of LAMC1 in GBM; (D) DFS of LAMC1 in GBM; (E) OS of LAMC1 in LGG; (F) DFS of LAMC1 in LGG; (G) OS of COL1A1 in LGG; and (H) DFS of COL1A1 in LGG. OS, overall survival; DFS, disease-free survival; GBM, glioblastoma; LGG, brain Lower Grade Gioma; COL1A1, collagen type I α1; LAMC1, laminin subunit γ1.

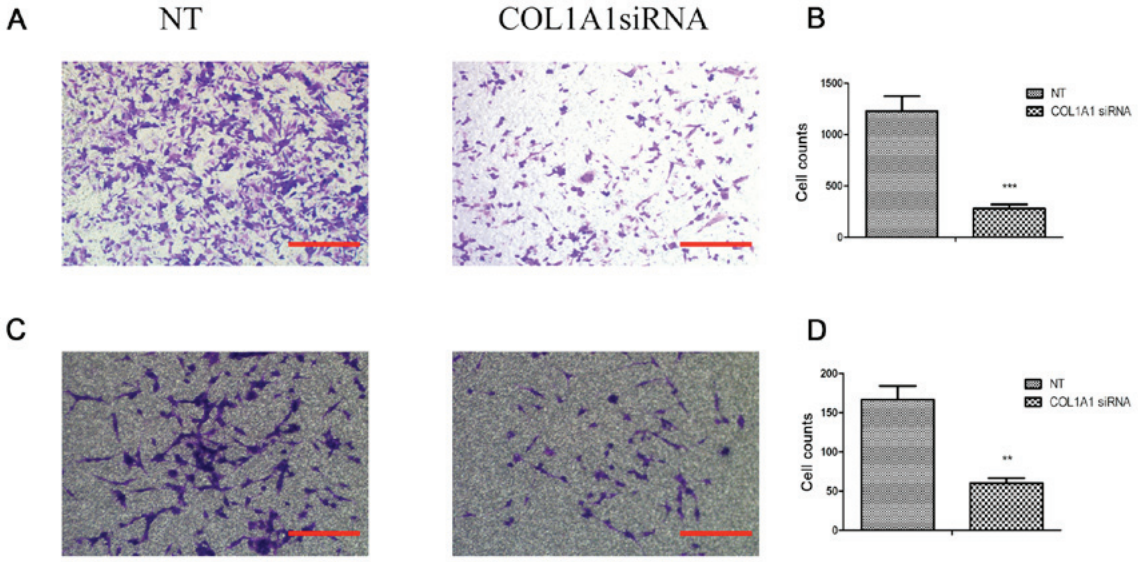

Figure 6. Transwell invasion assay was performed with U251MG and U87MG cells with or without COL1A1 siRNA treatment. (A and C) Representative micrographs (magnification, x100) of invaded cells in Transwell assays (plus Matrigel). Astrocytoma or glioblastoma cells ($1x10^4$) were seeded as indicated and co-cultured with COL1A1 siRNA for 24 h. (B and D) Graphic representation of the quantification of invaded cells. All data are presented as the means ± standard deviation of three independent experiments (scale bar, 100 μm). Data in (A and B) are from the U251MG cells, while those in (C and D) are from the U87MG cells. **P<0.01 and ***P<0.001. COL1A1, collagen type I α1.

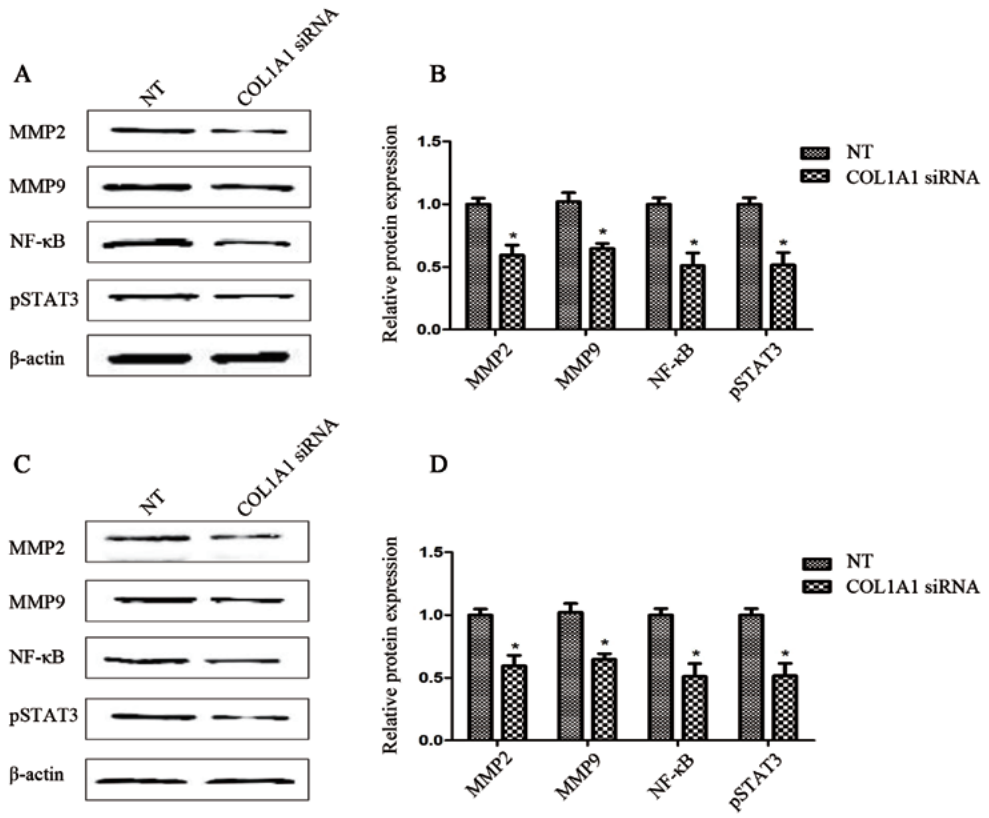

Figure 7. Inactive signaling pathways and the downregulation of genes and proteins associated with invasion. (A and C) Western blot analysis of protein lysates were prepared from control siRNA or COL1A1 siRNA. (B and D) Graphic representations of results of western blot analysis evaluating the changes in the invasion-related protein expression induced by COL1A1 siRNA treatment. Data in (A and B) are from the U251MG cells. Data in (C and D) are from the U87MG cells. *P<0.05. COL1A1, collagen type I α1.

In the present study, to increase the reliability of the results, gene expression profile data were downloaded from the microarrays GSE15824, GSE4290 and GSE19728, which all originated from 3 independent research object groups, from the GEO database. For comparisons with the normal brain, the upregulated DEGs of high-grade gliomas were organized, subjected to GO and KEGG pathway annotation, and used to construct the PPI network and for functional module analysis.

The results from these 2 technologies were comparable in terms of the ECM-related terms identified.

The ECM is comprised of a collection of extracellular molecules, including a mesh of fibrous proteins and glycosaminoglycans (GAGs), that are secreted by cells, providing the basis for cellular autonomy and cellular cooperation (28). The interactions between tumor cells and the host are key for the invasion of tumor cells (29). It has been previously reported that cell adhesion and migration in gliomas were increased by several ECM components, such as laminin (30,31) and collagen (32,33). The results of the present study support the notion that the ECM is important for the invasion of MA.

In addition, in this study, from the results of GO and KEGG analysis, it was indicated that cell adhesion and the PI3K/Akt signaling pathway may be of particular interest. Cell adhesion is a biological process through which cells interact and attach to ECM component or other cells. It is mediated by interactions between molecules on the cell surface and occurs via transmembrane cell adhesion molecules. Previous studies have demonstrated that a number of cell adhesion molecules are aberrantly expressed in gliomas and are involved in its malignant progression (34,35). The PI3K/Akt signaling pathway is a signal transduction pathway that promotes survival and growth in response to extracellular signals and it also plays an important role in the progression of tumors (36,37). Previous studies have revealed that the PI3K/Akt signaling pathway is abnormally expressed during malignant glioma progression (38) and alterations in the PI3K/Akt signaling pathway lead to glioma formation (39). The results of the present study confirm the association between cell adhesion and the PI3K/Akt signaling pathway and tumor invasion.

In order to further determine the tumor invasion-related molecules, the present study generated Venn diagrams to count the number of upregulated DEGs that existed in both WHO grades III and IV (FC value: IV>III), and those that were not presented in WHO grades I or II, in order to obtain the genes that were mostly associated with the malignant progression of tumor. A PPI network of the upregulated DEGs that existed in both WHO grades III and IV (FC value: IV>III), was created and analyzed using STRING and Cytoscape software; this allowed for the acquisition of genes that were in the most relevant module for MA invasion. Considering these two results, it was hypothesized that *COL1A1* and *LAMC1* may be the two most probable genes to be related to MA invasion.

COL1A1 is a key component of the ECM and plays an important role in cell adhesion and differentiation. A previous *in vitro* silencing experiment also demonstrated that COL1A1 was involved in GBM cell invasion (40). A recent study revealed that there was a higher expression of COL1A1 in GBM than in low-grade gliomas (6). By searching the Human Protein Atlas, the present study also observed that some MA tumor cells exhibited COL1A1 positive staining.

LAMC1 belongs to the laminins family of ECM glycoproteins. It has been reported that a high expression of LAMC1 together with a large GBM tumor size may be associated with a shorter median OS (41).

In order to further clarify the clinical significance of the abnormal changes in COL1A1 and LAMC, the present study utilized the Survival KM estimate on cBioportal TCGA online. The results demonstrated that COL1A1 was associated with the survival rate and recurrence in patients with MA, while LAMC1 was not. Of note, in patients with LGG, both LAMC1 and COL1A1 had significant effects on the survival KM curve. Therefore, it was concluded that, although COL1A1 and LAMC1 are closely related to MA invasion, their abnormal expression levels exert differential effects on patient survival and recurrence, which were also associated with the pathological levels in glioma patients. While COL1A1 exerted significant effects on the survival and recurrence of both GBM and LGG, the abnormal expression of LAMC1 only had significant effects on the survival and recurrence rate of LGG. In addition, using the above-mentioned bioinformatics approach, the present study revealed that *COL1A1* was the most likely invasion-related DEG in MA.

Bioinformatics analysis was applied to predict the functions of DEGs in MA; it was assumed that an assessment such as this should accompany several experimental parameters. The present study confirmed some of the aforementioned results through experiments using a cell model of MA. The expression of COL1A1 in the U251M cell line was associated with an increase in cell motility and invasiveness. An *in vitro* Transwell assay revealed that cells in which COL1A1 was knocked down were less invasive than the control cells. These results were consistent with those of the bioinformatics analysis, as well as those of the aforementioned previous studies. A recent study performed by Balbous *et al* (40), which aimed to identify a mesenchymal glioma stem cell profile, reported that the silencing of COL1A1 resulted in a significant reduction in cell invasive capabilities.

However, it is important to identify which signaling pathways are involved in COL1A1-induced glioma invasion. In this study, following a literature research, three signaling pathways, Janus kinase (JAK)/STAT3, PI3K/Akt and NF-κB, were identified to be closely related to glioma invasion.

When the JAK/STAT3 signaling pathway is activated, STAT3 is phosphorylated and p-STAT3 forms dimers that are then translocated to the nucleus. As a result, these activities may facilitate transcription and expression of genes related to the cell cycle (42), cell proliferation (43), invasion and metastasis (44). Furthermore, the cell invasive ability is known to have a close association with the degradation of ECM, and MMPs, which downstream of the PI3K/AKT signaling pathway, are also involved in these events. Previous studies have reported that there is an association between tumor invasion and the expression of MMP-2 and MMP-9 (45,46). Additionally, the sustained activation of NF-κB in gliomas has also been reported (47). The aberrant activation of NF-κB has been shown to play key roles in a range of biological behaviors, such as cell proliferation (48), angiogenesis (49), metastasis (50) and invasion (51). Of note, there is crosstalk between the three pathways. NF-κB signaling leads to MMP activation (52). JAK overexpression induces the activation of NF-κB, which frequently cooperates with STAT3 to upregulate metastasis, promoting genes such as MMPs and cytokines (53). As p-STAT3, NF-κB and MMPs are known to be crucial factors that may facilitate tumor invasion, it was hypothesized that they may also be involved in COL1A1-induced glioma cell invasion.

To text this hypothesis, in this study, experiments were designed and performed; key factors within these signaling

pathways were investigated by western blotting. The downregulation of COL1A1 in the U251MG or U87MG cells reduced the protein levels of the recognized invasion-related factors, such as p-STAT3, MMP-2, MMP-9 and NF-κB, suggesting that the JAK/STAT3, PI3K/AKT and NF-κB signaling pathways may be involved in COL1A1-mediated invasion.

The results of the present study are in agreement with those of a previous study that demonstrated that there was elevated COL1A1 expression in cancer (54). A previous *in vitro* study also suggested that COL1A1 activity may promote cancer cell proliferation and/or invasion (7). However, to the best of our knowledge, no studies to date have analyzed COL1A1 expression in gliomas, and as such, this may be one of the first reports. Unfortunately, the present study did not fully elucidate the mechanism underlying how COL1A1 affects these signaling pathways.

The identification of COL1A1 within gliomas provides the basis for future targeted treatments; the overexpression of COL1A1 facilitating cell invasion in glioma is a major therapeutic target. In the future, this may be a key prognostic factor for predicting OS.

Based on the high throughput data using bioinformatics technologies, the present study further investigated the MA microarray data. The results revealed that 'ECM', 'cell adhesion', and 'PI3K-Akt signaling pathway' were the most closely related GO or KEGG terms associated with MA invasion. In addition, further analysis highlighted *COL1A1* and *LAMC1* as major genes involved in MA invasion. Due to its correlation with the survival and recurrence of MA, COL1A1 may be a candidate biomarker for the prognosis and treatment of MA. Future experiments may provide evidence that COL1A1 may contribute to glioma invasion and participate in the JAK/STAT3, PI3K/Akt and NF-κB signaling pathways.

Acknowledgements

Not applicable.

Funding

This study was funded by the National Natural Science Research Foundation of China (grant no. 81772688). The writer would like to express his deep gratitude to the research team.

Availability of data and materials

The datasets used and/or analyzed during the current study are available from the corresponding author on reasonable request.

Authors' contributions

SS was involved in the conception and design of the study, project administration and drafted the manuscript; YWa performed most of the experiments and conducted the submission of the manuscript; YWu collected data from the internet, performed Bioinformatics analyses and organized the figures and tables; YG, QL, AAA, XFL and GQJ performed literature search. JG, LL, and FPW studied conception and design; YQL was involved in the conception and design of the study, and project supervision; DSG acquired the funding, was involved in the conception and design of the study, supervised the study and critically reviewed the manuscript. All authors have read and approved the final manuscript

Ethics approval and consent to participate

Not applicable.

Patient consent for publication

Not applicable.

Competing interests

The authors declare that they have no competing interests.

References

1. Van Meir EG, Hadjipanayis CG, Norden AD, Shu HK, Wen PY and Olson JJ: Exciting new advances in neuro-oncology: The avenue to a cure for malignant glioma. CA Cancer J Clin 60: 166-193, 2010.
2. Dolecek TA, Propp JM, Stroup NE and Kruchko C: CBTRUS statistical report: Primary brain and central nervous system tumors diagnosed in the United States in 2005-2009. Neuro-oncol 14 (Suppl 5): v1-v49, 2012.
3. Kulasingam V and Diamandis EP: Strategies for discovering novel cancer biomarkers through utilization of emerging technologies. Nat Clin Pract Oncol 5: 588-599, 2008.
4. Muhammad SA, Raza W, Nguyen T, Bai B, Wu X and Chen J: Cellular Signaling Pathways in Insulin Resistance-Systems Biology Analyses of Microarray Dataset Reveals New Drug Target Gene Signatures of Type 2 Diabetes Mellitus. Front Physiol 8: 13, 2017.
5. Wu YH, Chang TH, Huang YF, Huang HD and Chou CY: COL11A1 promotes tumor progression and predicts poor clinical outcome in ovarian cancer. Oncogene 33: 3432-3440, 2014.
6. Mustafa DA, Sieuwerts AM, Zheng PP and Kros JM: Overexpression of Colligin 2 in Glioma Vasculature is Associated with Overexpression of Heat Shock Factor 2. Gene Regul Syst Bio 4: 103-107, 2010.
7. Wang Q and Yu J: MiR-129-5p suppresses gastric cancer cell invasion and proliferation by inhibiting COL1A1. Biochem Cell Biol 96: 19-25, 2018.
8. Ilhan-Mutlu A, Siehs C, Berghoff AS, Ricken G, Widhalm G, Wagner L and Preusser M: Expression profiling of angiogenesis-related genes in brain metastases of lung cancer and melanoma. Tumour Biol 37: 1173-1182, 2016.
9. Gautier L, Cope L, Bolstad BM and Irizarry RA: affy - analysis of Affymetrix GeneChip data at the probe level. Bioinformatics 20: 307-315, 2004.
10. Sun L, Hui AM, Su Q, Vortmeyer A, Kotliarov Y, Pastorino S, Passaniti A, Menon J, Walling J, Bailey R, *et al*: Neuronal and glioma-derived stem cell factor induces angiogenesis within the brain. Cancer Cell 9: 287-300, 2006.
11. Grzmil M, Morin P Jr, Lino MM, Merlo A, Frank S, Wang Y, Moncayo G and Hemmings BA: MAP kinase-interacting kinase 1 regulates SMAD2-dependent TGF-β signaling pathway in human glioblastoma. Cancer Res 71: 2392-2402, 2011.
12. Liu Z, Yao Z, Li C, Lu Y and Gao C: Gene expression profiling in human high-grade astrocytomas. Comp Funct Genomics 2011: 245137, 2011.
13. Gentleman RC, Carey VJ, Bates DM, Bolstad B, Dettling M, Dudoit S, Ellis B, Gautier L, Ge Y, Gentry J, *et al*: Bioconductor: Open software development for computational biology and bioinformatics. Genome Biol 5: R80, 2004.
14. Lahti L, Torrente A, Elo LL, Brazma A and Rung J: A fully scalable online pre-processing algorithm for short oligonucleotide microarray atlases. Nucleic Acids Res 41: e110, 2013.
15. Ashburner M, Ball CA, Blake JA, Botstein D, Butler H, Cherry JM, Davis AP, Dolinski K, Dwight SS, Eppig JT, *et al*; The Gene Ontology Consortium: Gene ontology: Tool for the unification of biology. Nat Genet 25: 25-29, 2000.

16. Lomax J: Get ready to GO! A biologist's guide to the Gene Ontology. Brief Bioinform 6: 298-304, 2005.
17. Kanehisa M, Furumichi M, Tanabe M, Sato Y and Morishima K: KEGG: New perspectives on genomes, pathways, diseases and drugs. Nucleic Acids Res 45 (D1): D353-D361, 2017.
18. Dennis G Jr, Sherman BT, Hosack DA, Yang J, Gao W, Lane HC and Lempicki RA: DAVID: Database for Annotation, Visualization, and Integrated Discovery. Genome Biol 4: 3, 2003.
19. Szklarczyk D, Franceschini A, Wyder S, Forslund K, Heller D, Huerta-Cepas J, Simonovic M, Roth A, Santos A, Tsafou KP, *et al*: STRING v10: Protein-protein interaction networks, integrated over the tree of life. Nucleic Acids Res 43 (D1): D447-D452, 2015.
20. Shannon P, Markiel A, Ozier O, Baliga NS, Wang JT, Ramage D, Amin N, Schwikowski B and Ideker T: Cytoscape: A software environment for integrated models of biomolecular interaction networks. Genome Res 13: 2498-2504, 2003.
21. Bader GD and Hogue CW: An automated method for finding molecular complexes in large protein interaction networks. BMC Bioinformatics 4: 2, 2003.
22. Bindea G, Mlecnik B, Hackl H, Charoentong P, Tosolini M, Kirilovsky A, Fridman WH, Pagès F, Trajanoski Z and Galon J: ClueGO: A Cytoscape plug-in to decipher functionally grouped gene ontology and pathway annotation networks. Bioinformatics 25: 1091-1093, 2009.
23. Bindea G, Galon J and Mlecnik B: CluePedia Cytoscape plugin: Pathway insights using integrated experimental and in silico data. Bioinformatics 29: 661-663, 2013.
24. Uhlén M, Fagerberg L, Hallström BM, Lindskog C, Oksvold P, Mardinoglu A, Sivertsson Å, Kampf C, Sjöstedt E, Asplund A, *et al*: Proteomics. Tissue-based map of the human proteome. Science 347: 1260419, 2015.
25. Cerami E, Gao J, Dogrusoz U, Gross BE, Sumer SO, Aksoy BA, Jacobsen A, Byrne CJ, Heuer ML, Larsson E, *et al*: The cBio cancer genomics portal: An open platform for exploring multidimensional cancer genomics data. Cancer Discov 2: 401-404, 2012.
26. Cancer Genome Atlas Research Network: Comprehensive genomic characterization defines human glioblastoma genes and core pathways. Nature 455: 1061-1068, 2008.
27. Loging WT, Lal A, Siu IM, Loney TL, Wikstrand CJ, Marra MA, Prange C, Bigner DD, Strausberg RL and Riggins GJ: Identifying potential tumor markers and antigens by database mining and rapid expression screening. Genome Res 10: 1393-1402, 2000.
28. Michel G, Tonon T, Scornet D, Cock JM and Kloareg B: The cell wall polysaccharide metabolism of the brown alga Ectocarpus siliculosus. Insights into the evolution of extracellular matrix polysaccharides in Eukaryotes. New Phytol 188: 82-97, 2010.
29. Pauli BU, Schwartz DE, Thonar EJ and Kuettner KE: Tumor invasion and host extracellular matrix. Cancer Metastasis Rev 2: 129-152, 1983.
30. Goldbrunner RH, Haugland HK, Klein CE, Kerkau S, Roosen K and Tonn JC: ECM dependent and integrin mediated tumor cell migration of human glioma and melanoma cell lines under serum-free conditions. Anticancer Res 16 (6B): 3679-3687, 1996.
31. Ljubimova JY, Fujita M, Khazenzon NM, Ljubimov AV and Black KL: Changes in laminin isoforms associated with brain tumor invasion and angiogenesis. Front Biosci 11: 81-88, 2006.
32. Senner V, Ratzinger S, Mertsch S, Grässel S and Paulus W: Collagen XVI expression is upregulated in glioblastomas and promotes tumor cell adhesion. FEBS Lett 582: 3293-3300, 2008.
33. Maestro RD, Shivers R, McDonald W and Maestro AD: Dynamics of C6 astrocytoma invasion into three-dimensional collagen gels. J Neurooncol 53: 87-98, 2001.
34. Izumoto S, Ohnishi T, Arita N, Hiraga S, Taki T and Hayakawa T: Gene expression of neural cell adhesion molecule L1 in malignant gliomas and biological significance of L1 in glioma invasion. Cancer Res 56: 1440-1444, 1996.
35. Wang YB, Hu Y, Li Z, Wang P, Xue YX, Yao YL, Yu B and Liu YH: Artemether combined with shRNA interference of vascular cell adhesion molecule-1 significantly inhibited the malignant biological behavior of human glioma cells. PLoS One 8: e60834, 2013.
36. Osaki M, Oshimura M and Ito H: PI3K-Akt pathway: its functions and alterations in human cancer. Apoptosis 9: 667-676, 2004.
37. Cantley LC and Neel BG: New insights into tumor suppression: PTEN suppresses tumor formation by restraining the phosphoinositide 3-kinase/AKT pathway. Proc Natl Acad Sci USA 96: 4240-4245, 1999.
38. Choe G, Horvath S, Cloughesy TF, Crosby K, Seligson D, Palotie A, Inge L, Smith BL, Sawyers CL and Mischel PS: Analysis of the phosphatidylinositol 3'-kinase signaling pathway in glioblastoma patients in vivo. Cancer Res 63: 2742-2746, 2003.
39. Yuan TL and Cantley LC: PI3K pathway alterations in cancer: Variations on a theme. Oncogene 27: 5497-5510, 2008.
40. Balbous A, Cortes U, Guilloteau K, Villalva C, Flamant S, Gaillard A, Milin S, Wager M, Sorel N, Guilhot J, *et al*: A mesenchymal glioma stem cell profile is related to clinical outcome. Oncogenesis 3: e91, 2014.
41. Huang SX, Zhao ZY, Weng GH, He XY, Wu CJ, Fu CY, Sui ZY, Zhong XM and Liu T: The correlation of microRNA-181a and target genes with poor prognosis of glioblastoma patients. Int J Oncol 49: 217-224, 2016.
42. Sainz-Perez A, Gary-Gouy H, Gaudin F, Maarof G, Marfaing-Koka A, de Revel T and Dalloul A: IL-24 induces apoptosis of chronic lymphocytic leukemia B cells engaged into the cell cycle through dephosphorylation of STAT3 and stabilization of p53 expression. J Immunol 181: 6051-6060, 2008.
43. Zhang Y, Jia Y, Li P, Li H, Xiao D, Wang Y and Ma X: Reciprocal activation of α5-nAChR and STAT3 in nicotine-induced human lung cancer cell proliferation. J Genet Genomics 44: 355-362, 2017.
44. Sp N, Kang DY, Kim DH, Park JH, Lee HG, Kim HJ, Darvin P, Park YM and Yang YM: Nobiletin Inhibits CD36-Dependent Tumor Angiogenesis, Migration, Invasion, and Sphere Formation Through the Cd36/Stat3/Nf-Kb Signaling Axis. Nutrients 10: 10, 2018.
45. Liabakk NB, Talbot I, Smith RA, Wilkinson K and Balkwill F: Matrix metalloprotease 2 (MMP-2) and matrix metalloprotease 9 (MMP-9) type IV collagenases in colorectal cancer. Cancer Res 56: 190-196, 1996.
46. Sugiura Y, Shimada H, Seeger RC, Laug WE and DeClerck YA: Matrix metalloproteinases-2 and -9 are expressed in human neuroblastoma: Contribution of stromal cells to their production and correlation with metastasis. Cancer Res 58: 2209-2216, 1998.
47. Nagai S, Washiyama K, Kurimoto M, Takaku A, Endo S and Kumanishi T: Aberrant nuclear factor-kappaB activity and its participation in the growth of human malignant astrocytoma. J Neurosurg 96: 909-917, 2002.
48. Huang F, Xiong X, Wang H, You S and Zeng H: Leptin-induced vascular smooth muscle cell proliferation via regulating cell cycle, activating ERK1/2 and NF-kappaB. Acta Biochim Biophys Sin (Shanghai) 42: 325-331, 2010.
49. Ni H, Zhao W, Kong X, Li H and Ouyang J: Celastrol inhibits lipopolysaccharide-induced angiogenesis by suppressing TLR4-triggered nuclear factor-kappa B activation. Acta Haematol 131: 102-111, 2014.
50. Hsiao YT, Fan MJ, Huang AC, Lien JC, Lin JJ, Chen JC, Hsia TC, Wu RS and Chung JG: Deguelin Impairs Cell Adhesion, Migration and Invasion of Human Lung Cancer Cells through the NF-[Formula: See text]B Signaling Pathways. Am J Chin Med 46: 209-229, 2018.
51. Zhang J, Xu YJ, Xiong WN, Zhang ZX, Du CL, Qiao LF, Ni W and Chen SX: Inhibition of NF-kappaB through IkappaBalpha transfection affects invasion of human lung cancer cell line A549. Ai Zheng 27: 710-715, 2008 (In Chinese).
52. Shihab PK, Al-Roub A, Al-Ghanim M, Al-Mass A, Behbehani K and Ahmad R: TLR2 and AP-1/NF-kappaB are involved in the regulation of MMP-9 elicited by heat killed Listeria monocytogenes in human monocytic THP-1 cells. J Inflamm (Lond) 12: 32, 2015.
53. Teng Y, Ross JL and Cowell JK: The involvement of JAK-STAT3 in cell motility, invasion, and metastasis. JAK-STAT 3: e28086, 2014.
54. Liu S, Liao G and Li G: Regulatory effects of COL1A1 on apoptosis induced by radiation in cervical cancer cells. Cancer Cell Int 17: 73, 2017.